

Comparative studies of passive imaging in terahertz and mid-wavelength infrared ranges for object detection

M. Kowalski, M. Kastek

Abstract— We compared the possibility of detecting hidden objects covered with various types of clothing by using passive imagers operating in a terahertz (THz) range at 1.2 mm (250 GHz) and a mid-wavelength infrared (MWIR) at 3–6 μm (50–100 THz). We investigated theoretical limitations, performance of imagers, and physical properties of fabrics in both regions. In order to investigate the time stability of detection, we performed measurements in sessions each lasting 30 minutes. We present a theoretical comparison of two spectra, as well as the results of experiments. In order to compare capabilities of passive imaging of hidden objects, we combined properties of textiles, performance of imagers, and properties of radiation in both spectral ranges. The paper presents the comparison of the original results of measurement sessions for the two spectrums with analysis.

Index Terms— terahertz, mid-infrared, multispectral imaging, object detection, screening camera, textile

I. INTRODUCTION

Security and surveillance systems are one of the most challenging applications for infrared (IR) and terahertz (THz) imagers. The main aim of imagers is to deliver high quality images of targets of interest. One of the major challenges in this field is ability to automatically reveal objects placed on the surface of human body and covered with clothing. Terahertz imagers, which seem to be the best solution, very often provide images with low signal-to-noise ratio, low spatial resolution, and offer limited distance of imaging. A reasonable alternative seems to be an infrared camera.

The most useful properties of imagers operating in infrared and terahertz ranges are the ability to detect small temperature differences on the object's surface, as well as the ability to see through clothing, respectively. Both properties of imagers can be used to detect objects such as weapons or explosives concealed under clothing.

A classic approach to detection of hidden objects is to use metal detectors, X-ray scanners and manual searching.

Active full body X-ray scanners offer pictures with a very

M. Kowalski, is with Institute of Optoelectronics, Military University of Technology, Gen. S. Kaliskiego 2 Str., 00-908 Warsaw, Poland (e-mail: marcin.kowalski@wat.edu.pl).

M. Kastek, is with Institute of Optoelectronics, Military University of Technology, Gen. S. Kaliskiego 2 Str., 00-908 Warsaw, Poland (e-mail: mariusz.kastek@wat.edu.pl).

good resolution and performance [1]. However, they are forbidden in European Union due to their harmful impact on human bodies.

The imagers presented in this study are supposed to be non-intrusive because they use non-ionizing types of radiation. In this study we focus on passive cameras operating in terahertz and mid-wavelength infrared spectral ranges.

Terahertz radiation covers frequencies from 0.1 THz to 10 THz (wavelengths from 3 mm to 30 μm) and is commonly referred to as far-infrared [2-4]. Terahertz full-body scanners typically operate below 1 THz [5-8]. The most valuable property of the terahertz radiation is that these waves can penetrate fabrics and other materials [9-11] with low water content. Another valued property is that because this radiation is low-energetic it does not ionize matter so it is not harmful to people. Both properties established terahertz radiation as suitable for screening people, particularly for remote detection of dangerous objects [12-14].

Infrared is radiation typically comprised in the range between 0.7 μm and 30 μm (430 THz down to 10 THz) [15]. Commonly, infrared is divided into four sections: near, short-wavelength, mid-wavelength, long-wavelength and far-infrared. Mid-wavelength infrared (MWIR) is a part of electromagnetic spectrum covering wavelengths from 3 μm to 8 μm (100 down to 37.5 THz). Devices operating in the MWIR range are able to detect small differences of temperature [16] on an object's surface, therefore are useful in searching for concealed objects covered with various types of fabrics [17-19].

The fundamental measures for assessing performance of terahertz and infrared imagers are minimum resolvable temperature difference (MRTD) and noise-equivalent temperature difference that describe ability to differentiate temperatures [19]. These parameters influence the camera's potential to detect objects covered with clothing. Typical values of NETD are between 40 and 130 mK for cameras equipped with uncooled detectors and between 20 mK -70 mK for cooled detectors. Performance of THz imagers in the meaning of NETD value is lower and, typically, those values are in the range between 0.5 K and 5 K.

We present comparative studies of imaging possibilities of objects covered with common textiles in the terahertz (250 GHz) and MWIR (3-8 μm) ranges using state-of-the-art equipment. We conducted a theoretical analysis in two basic aspects: power relationship between spectral bands, and relationship between heat transfer through clothing and between a hidden object and a human body. In order to verify

the theoretical studies, we measured the transmittance of radiation through several textiles in both spectral bands and we performed experiments using state-of-the-art cameras. Hereby, we present the analysis of the studies' results.

II. THEORY OF HIDDEN OBJECTS DETECTION IN PASSIVE MODE

Imagers operating in passive mode register radiation emitted by objects do not require additional illuminators. Cameras operating in both mid-wavelength infrared and terahertz range register radiation proportional to the relative distribution of the apparent temperature of objects placed in the field of view of the camera lens. The projection of objects depends on parameters of camera and lens, as well as on temperature difference between objects and their emissivity.

In order to conduct a theoretical analysis of hidden objects' detection possibility, we used Planck's law. According to it, each body being in the thermal equilibrium emits the radiation in a broad spectral range [20]. It means that each body emits radiation in both infrared and terahertz frequencies. The amount of energy radiated by a body is described by equation 1. The critical difference between the detection at terahertz frequencies and the infrared detection is the photon energy (at 300 GHz = 1.24 meV, compared with the energy of 124 meV at 10 μm) and the spectral radiance described by the formula [20]:

$$B_\nu(T) = \frac{2 \cdot \nu^2}{c^2} k \cdot T \quad (1)$$

where k is the Boltzmann constant and T is the temperature, at 300 GHz $B_\nu(T) = 8.28 \cdot 10^{-33} \cdot W / sr \cdot m^2$, compared with the $B_\nu(T) = 3.31 \cdot 10^{-10} \cdot W / sr \cdot m^2$ at 5 μm.

In the paper we consider objects like guns and knives placed on the human body. Since both a human body and an object are in a direct contact, the energy (heat) is transferred between the human body and the concealed object by transmission of heat between those two bodies. The heat conduction is described by Fourier's law which states that time rate of a heat transfer through a material is proportional to the negative gradient in the temperature and to the area, at right angles to that gradient, through which the heat flows [21].

$$\vec{q} = -k\nabla T \quad (2)$$

where \vec{q} is the local heat flux density, k is the material's conductivity (related to temperature) and ∇T is the temperature gradient. The Fourier's law of thermal conduction is often simplified and presented in one dimensional form of [21]

$$q_x = -k \frac{dT}{dx} \quad (3)$$

The energy radiated from the human body to the object is emitted according to the Planck's law in a broad spectral range, including THz and IR frequencies. The possibility of distinguishing temperature values on the object's surface by passive cameras (MWIR and terahertz) can be described in an analogous way. The temperature differences on the surface correspond to the differences of energy radiated in the whole radiation range. Passive cameras assign temperature differences to differences in the radiated energies in their spectral ranges per unit surface.

In order to detect an object concealed under clothing, difference between the total luminance of the observed surface covering the object and the nearest neighboring area should be sufficient. We can consider a layer of clothing as a porous material, partly transmitting thermal radiation. Depending on the structure of a fabric, thermal radiation can be partly transmitted through holes in the fabric's matrix. The remaining thermal radiation is transmitted as through an optical filter [20]. Such a filter is described by emissivity ϵ , reflectance ρ and transmittance τ . Radiation from such a material depends on a temperature of the surface layer. This temperature lies, in fact, between temperature of the inner and outer sides of the fabric [20]. To estimate a limiting value of the contrast, we assumed that for any fabric the temperature of the surface emitting thermal radiation equaled temperature of the human body or the detected object.

The radiant exitance value Φ_W in the adjacent area W that differs from the radiant exitance Φ_S , of the neighboring area S (Fig. 1) is modified by an object covered with clothing. Contour lines indicate the compared areas of identical size. Figure 1a shows the thermal image with marked regions of interest (ROIs): red – the hidden pistol area, green – the randomly selected area with the size and shape of the pistol. Temperatures of these ROIs have been used to calculate the values necessary to determine effectiveness of detecting the concealed object [22]. Elements of total radiant exitance from both W and S surfaces are presented in Fig. 1. These components include emission from clothing, body, and hidden object, with transmissive properties of the clothing taken into account.

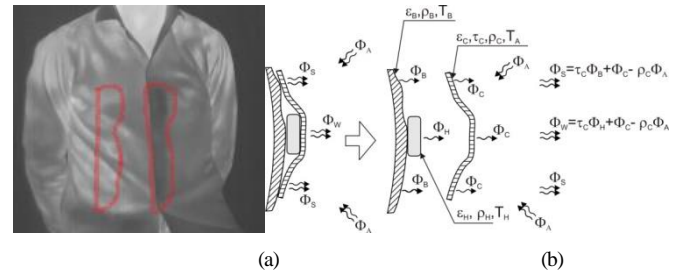


Fig. 1. (a) Thermal image of clothing surface with and without any object, (b) thermal radiation model.

In order to estimate thermal contrast based on the analysis of the image, a simplified model has been adopted in which radiant exitances Φ_S and Φ_W (of areas without and with a hidden object underneath, respectively) are given by the following equations [21]:

$$\Phi_S = \tau_C \Phi_B + \Phi_C + \rho_C \Phi_A \quad (4)$$

$$\Phi_W = \tau_C \Phi_H + \Phi_C + \rho_C \Phi_A \quad (5)$$

where ρ_C is the reflection coefficient of a clothing fabric, τ_C its transmittance coefficient, Φ_B - the radiant exitance of human skin, Φ_C - the radiant exitance of a clothing fabric, Φ_A - the irradiance of the clothing surface, and Φ_H - the radiant exitance of a hidden object. Each component of both equations (4) and (5) presents different physical phenomena. Component $\rho_C \Phi_A$ describes the ambient radiation reflected from the clothing surface, $\tau_C \Phi_B$ is the portion of skin radiation emerging through a fabric characterized by the transmittance coefficient τ_C , whereas $\tau_C \Phi_H$ is the portion of radiation from a hidden object that passes through the same

fabric. In both relations (4) and (5) we assumed that temperature of the fabric surface which results in the radiation component Φ_C is close to the ambient temperature T_A . Another assumption that this temperature was approximately the same for all the surfaces of the clothing under consideration (shirt, T-shirt, sweater) was adopted. The energetic contrast K between neighbour areas W and S in thermal equilibrium can be described as [21]:

$$K = \frac{\Phi_S - \Phi_W}{\Phi_S} = \frac{(\tau_C \Phi_B + \Phi_C + \rho_C \Phi_A) - (\tau_C \Phi_H + \Phi_C + \rho_C \Phi_A)}{\tau_C \Phi_B + \Phi_C + \rho_C \Phi_A} = \frac{\tau_C (\Phi_B - \Phi_H)}{\tau_C \Phi_B + \Phi_C + \rho_C \Phi_A} \quad (6)$$

The conducted analysis revealed that the relation between the exitance transmitted through the hidden object coming from the body to exitance of the W surface is negligible in both spectral ranges. Therefore, the analysis presented above does not take into account the transmittance coming from the human body that was transmitted, absorbed and re-emitted by the hidden object. We assumed that temperature of the surface observed with imagers equalled the temperature of the solid state in contact with a corresponding material. This assumption allows to estimate the maximum obtainable contrast for the hidden objects relative to their surroundings and overestimated the calculated values of the contrast because materials used for clothing manufacture do not conduct heat perfectly. As a result, the actual temperature of the subsurface layer was lower than the value adopted for the estimation.

The analysis presented above can be written for spectrally-related parameters. In order to connect wavelength and temperature we used the function describing the spectral contrast for a given wavelength $cp(\lambda, T)$ and temperature (T). The relationship can be described by the following equation [22]:

$$cp(\lambda, T) = \frac{\phi_B(\lambda, T) - \phi_H(\lambda, T)}{\phi_B(\lambda, T)} \quad (7)$$

where $\phi_B(\lambda, T)$ is the spectral radiant exitance of a human body, and $\phi_H(\lambda, T)$ is the spectral radiant exitance of a hidden object. The values of the spectral radiant exitances of a body, as well as an object can be described by [22]:

$$\phi_B(\lambda, T) = \varepsilon_B(\lambda, T) \cdot m_{BB}(\lambda, T) \quad (8)$$

$$\phi_H(\lambda, T) = \varepsilon_H(\lambda, T) \cdot m_{BB}(\lambda, T) \quad (9)$$

where $\varepsilon_B(\lambda, T)$, $\varepsilon_H(\lambda, T)$ and $m_{BB}(\lambda, T)$ are the spectral emissivity of a human body, the spectral emissivity of a hidden object and the spectral radiant exitance of a blackbody, respectively.

Real imagers operating in the infrared and terahertz ranges have a finite spectral range of $\Delta\lambda = \lambda_{\max} - \lambda_{\min}$ that is determined by the detector spectral response and transmittance characteristics of the

applied optics. However, it is possible, for a given spectral band $\Delta\lambda$, ambient temperature T_A , body temperature T_B and temperature of a hidden object T_H to define the power contrast $CP(\lambda_{\min}, \lambda_{\max}, T_A, T_B, T_H)$ given by the following [22]:

$$CP(\lambda_{\min}, \lambda_{\max}, T_A, T_B, T_H) = \frac{\int_{\lambda_{\min}}^{\lambda_{\max}} \tau_C(\lambda, T_A) \varepsilon_H(\lambda, T_H) m_{BB}(\lambda, T_H) d\lambda}{\int_{\lambda_{\min}}^{\lambda_{\max}} \tau_C(\lambda, T_A) \varepsilon_B(\lambda, T_B) m_{BB}(\lambda, T_B) d\lambda} \quad (10)$$

where $\tau_C(\lambda, T)$ is the spectral transmittance coefficient of the clothing. The calculated power contrast for the spectral range of 3–6 μm is presented in Fig. 2. The results correspond to calculations made for different values of the average temperature, determined for each ROI at equal time intervals (5 minutes). In this way, the change in the power contrast value over time was determined.

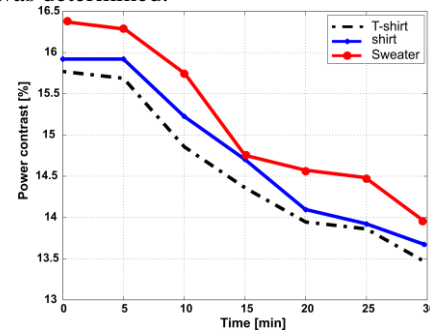


Fig. 2. Calculation of power contrast for a T-shirt (green line), shirt (blue line) and sweater (red line) within the MWIR (3–6 μm) range.

Two bodies directly connected strive to achieve thermodynamic equilibrium. Temperature of both of them within a certain time is equalized. In the case where one body has a constant temperature (human body) and the other lower ambient temperature, both bodies will tend to balance. As a result the second body is heated by taking energy from the first body. This situation causes that the above analysis should be repeated at intervals.

III. TRANSMITTANCE OF COATING MATERIALS

To detect an object covered with textiles using a camera means to make the textile invisible. In both spectrums we visualize the spatial distribution of radiation. When we visualize the object covered with clothes, the amount of radiation reaching the camera's detector depends inter alia on transmission of textiles covering the object. In order to describe the process of imaging objects covered with fabric, we investigated the radiation transmittance through coating materials.

One of terahertz radiation properties is ability to penetrate various fabrics [23]. In order to provide a database for statistical studies, we measured transmittance of 46 covering materials with different compositions and different basic weights, within both terahertz and infrared ranges. Measurements were made

by using a TPS Spectra 3000 time-domain (THz) spectrometer from TeraView [24] and a VERTEX 80V Fourier-transform infrared (FTIR) spectrometer from Bruker [25].

The measurement results for popular fabrics' transmittance indicated that the transmittance of terahertz radiation through a fabric decreases with increasing frequency and basic weight. The transmittance depends on fabric type, basic weight and its thickness (number of layers). We measured the transmittance of clothing materials within the frequency range of 150 GHz to 2.5 THz. The maximum value of radiation transmittance through a fabric is at the frequency of 150 GHz.

It should be noted that 92% of the tested fabric exhibited transmittance greater than 20% within the range of 150 GHz to 1 THz. This result indicates that body scanners should operate at the frequency below 1 THz. Some of the fabric had a transmittance of 20%, even for frequencies near 2 THz. This group consists of fabric containing polyester and viscose.

Cotton and polyester are one of the most popular materials for clothing. Graphs of transmittance through samples of canvas made of a composition of cotton and polyester with different basic weights are presented in Fig. 3. The graph presents the trend that the radiation transmittance decreases with increasing basic weight. The transmittance through a composition of cotton and polyester for frequencies above 1 THz is significantly lower than for 250 GHz.

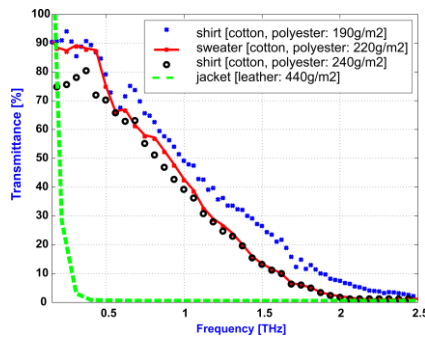


Fig. 3. Transmittance through canvas with different basic weights. Blue crosses show a shirt made of cotton and polyester, 190 g/m², single layer; red crosses show a sweater made of cotton and polyester, 220 g/m²; black circles show a shirt made of cotton and polyester, show 240 g/m², single layer; solid blue lines show a leather jacket 440 g/m², single layer.

The median value for the transmittance through 46 clothing materials at the frequency of 250 GHz was 89.05%. Transmittance of infrared radiation through fabrics is commonly known as very low [15, 23, 26]. The results of our measurements obtained using a Fourier Transform Infrared spectrometer confirmed this thesis. The statistics for the measured fabrics for 3 μm and 5 μm are presented in Table 1. The median value, as well as the maximum value of transmittance is decreasing with increasing wavelength. However, the median value which is 0.425 for 3 μm and 0.290 for 5 μm indicates that the transmittance is significantly low. This also means that we cannot detect objects covered with clothing due to a high transmittance as we do in the terahertz range. Concealed objects' detection capabilities of imagers operating in the MWIR range are based on a direct heat transfer between body, object and clothing.

TABLE I

TRANSMITTANCE [%] OF RADIATION THROUGH SELECTED COATING MATERIALS FOR THE CHOSEN WAVELENGTHS.

| Material | 3 μm [%] | 5 μm [%] |
|----------------|----------|----------|
| MAX: | 48.349 | 35.102 |
| MEDIAN: | 0.425 | 0.290 |

Graphs of transmittance through popular coating materials are presented in Fig. 4.

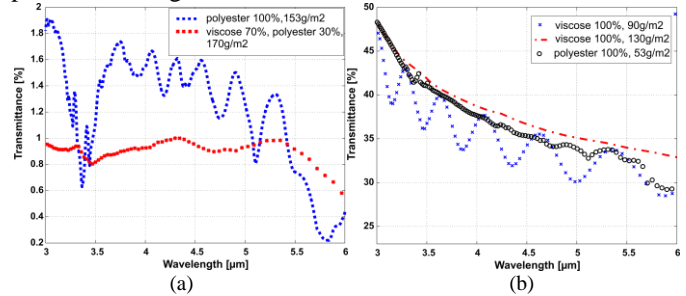


Fig. 4. Transmittance of mid-wavelength infrared through various materials. (a) Solid blue line shows 100% polyester, 153 g/m²; broken red line shows 70% viscose, 30% polyester, 170 g/m². (b) Blue crosses show viscose 100%, 90 g/m²; red dots show viscose 100%, 130 g/m²; black circles show polyester 100% 53 g/m².

Analysis of graphs presented in Fig. 4(b), as well as maximum values shown in Table 1 indicate that some fabrics have a very high transmittance in the MWIR range. These fabrics typically have basic weight smaller than 130 g/cm². The maximum values were more than 20 times greater than the mean values. Graphs of transmittance through four chosen fabrics with high transmittance values are presented in Fig. 4(b).

In order to hide an object under clothing, a fabric used to mask the object should be non-transparent to visible light. This condition is satisfied with fabrics with a relatively high basic weight. Transmittance through low basic weight fabrics presented in Fig. 5(b) within the range of 3–6 μm was very high, up to 48%.

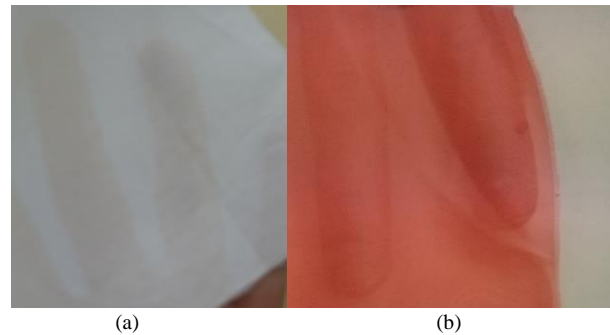


Fig. 5. Images of fingers covered with canvas of (a) viscose 100%, 90 g/m², (b) polyester 100% 53 g/m².

However, images of fingers covered with canvas made of viscose 100%, (basic weight of 90 g/m²) and polyester 100% (basic weight of 53 g/m²), presented in Fig. 5 indicate that these fabrics are semi-transparent to visible light. The fingers covered by these canvas are easily visible in the visible range, therefore, their masking capabilities are questionable.

IV. MEASUREMENTS' ENVIRONMENT

In order to compare capabilities of concealed objects' detection within the mid-wavelength infrared and terahertz ranges, as well as to verify the theoretical analysis, we employed imagers, performed experiments and prepared a measurement methodology. During the experiments we simultaneously acquired images of the same scene. In order to assess properties' changes for detection of hidden objects in time, experiments were divided into sessions lasting 30 minutes each. During every second, THz and LWIR imagers acquired 30 and 6 frames respectively. The frame rates of both imagers are suitable for stand-off imaging as well as for in-motion imaging. The goal of long lasting measurements sessions was to assess how changes of objects' temperature affect detection performance in both spectrums. The measurement methodology employed during measurements consisted of methods and algorithms, as well as the hardware setup. The theoretical analysis was verified using various objects covered with various types of fabric.

In order to collect all the necessary data, the measurement setup consisted of two passive commercially available cameras, a thermo-hygrometer (to control air humidity and ambient temperature) and two thermo-elements (to control temperatures of the human body and the object). To provide the measurement scene with a controllable and uniform background, a photographic shield was used. A schematic of the measurement setup is presented in Fig. 6.

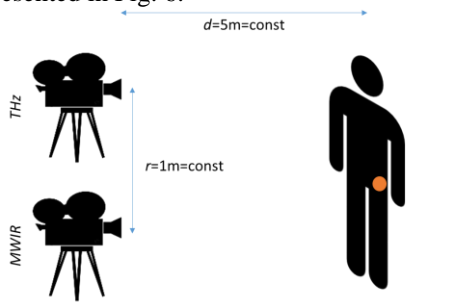


Fig. 6. Measurement setup.

To investigate the possibility of detecting a hidden object in the terahertz and infrared ranges, a TS4 imager (Digital Barriers, ThruVision) [27] and a mid-wavelength infrared (MWIR) camera (FLIR Systems Inc.) [28] were used. The parameters for the measurement equipment used during laboratory measurements are presented in Table 2.

The process of detection of objects covered with fabrics relies on the analysis of a two-dimensional distribution of the relative temperature of objects in the camera's lens field of view, as well as on the transmittance through clothing. The relative temperature between the object and the body changes during the experiment as a consequence of energy transmission between them. Assuming that the object is hidden under clothing for a specified period of time, and its initial temperature is lower than the body's, it is heated by the body, and the object and the body reach thermal equilibrium. In order to assess the impact of temperature changes on the capability of detection we performed the measurements in 30 minute sessions. During each session a single configuration with a set of clothes and objects was investigated.

TABLE II
MEASUREMENT EQUIPMENT

| Types of Systems | Parameters | |
|---|---------------------------------------|---|
| MWIR Camera SC5600 (Flir Systems) | Detection unit | FPA (focal plane array), 640 × 512 pixels, InSb cooled |
| | Field of View (FOV) spectral range | 20° × 15° 3 μm ÷ 5 μm |
| | NETD | 20 mK |
| THz camera TS4 (ThruVision) | Detection unit | passive sensing line, 124 × 271 pixels uncooled |
| | Frequency, bandwidth NETD | 0.25 THz ± 20 GHz (1.11 mm ÷ 1.3 mm) ~1 K |

During the experiments the distance between the human (stationary) carrying the object and the cameras was constant (5 m), the ambient temperature was constant (294 K, controlled by the air conditioning) and the relative humidity varied by 3%. Measurement data (images, air temperature, humidity and pressure, values of the body and object temperatures) were collected every 5 minutes. We employed two kinds of objects during the measurement session - a metal knife and a plastic pistol (Fig. 7).

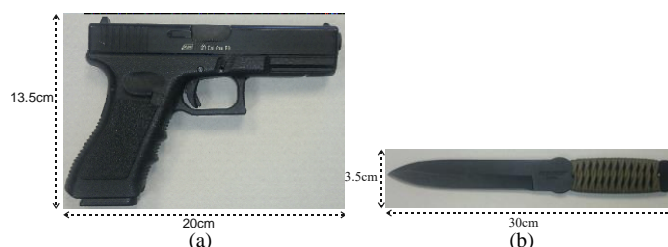


Fig. 7. Test objects used during the experiments: (a) plastic pistol, (b) metal knife.

The test objects, presented in Fig. 7, were combined with various types of clothing of different composition. Graphs of the transmittance through the clothing used during experiments are presented in Fig. 8.

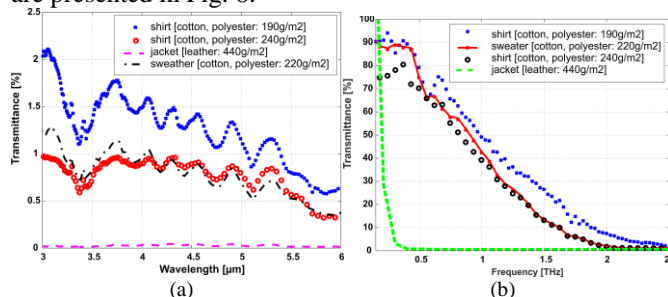


Fig. 8. Transmittance of infrared (a) and terahertz (b) radiation through different clothes.

Figure 8 presents the graphs of transmittance through two shirts and a sweater made of cotton and polyester with different basic weight and leather jacket within the MWIR (3–6 μm) and THz (150 GHz–2.5 THz) ranges. All the presented graphs confirm the trend that the transmittance through clothing within the infrared and terahertz range decreases with increasing basic weight. Moreover, the transmittance of terahertz radiation is significantly greater than of infrared radiation.

V. RESULTS AND ANALYSIS

Figures 9-12 present results of the selected measurement sessions. Presented images were recorded with the MWIR and terahertz cameras. During the measurement sessions two types of test objects (plastic pistol and metal knife) and one type of clothing were used. Images are arranged in groups of three presenting images acquired in specified time intervals; at the beginning of the experiment, and after 15 and 30 minutes. We collected the experimental data from the imagers, thermo-elements and hygrometer and two cameras every 5 minutes.

The first six images shown in Figs. 9 and 10 present a person with a metal knife hidden under shirt. In order to investigate the impact of a heat transfer between the human body and the hidden object, the test objects and clothes were allowed to reach thermal equilibrium with the environment before starting the experiments. Just before the experiments thermocouples were attached to the measured surfaces with an elastic adhesive tape that provided good thermal contact with the surface. The K-type thermocouples with a jacket diameter of 0.5 mm as temperature sensors were used.

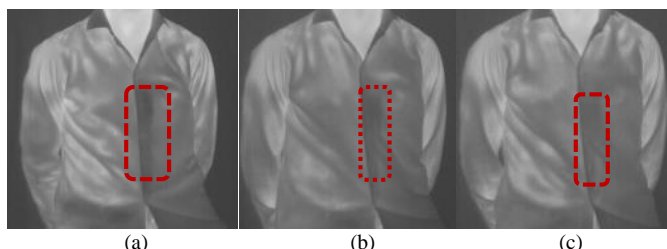


Fig. 9. MWIR images presenting a man wearing a shirt, with metal knife at the beginning of the measurement (a), after 15 minutes (b) and after 30 minutes (c).

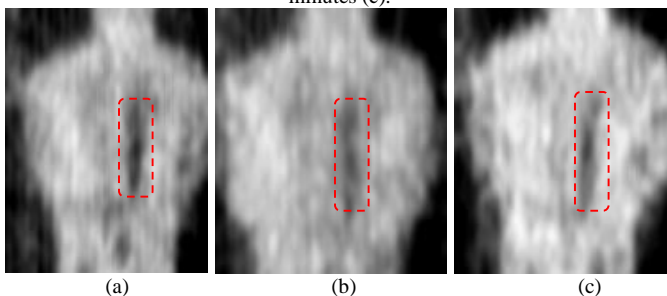


Fig. 10. THz images presenting a man wearing a shirt, with metal knife at the beginning of the measurement (a), after 15 minutes (b) and after 30 minutes (c).

Images shown in Figs. 12 and 13 present a person with the plastic gun dressed with a shirt.

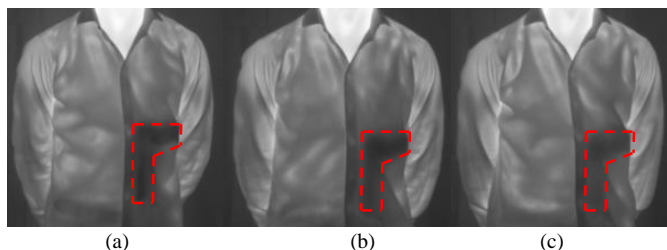


Fig. 11. MWIR images presenting a man wearing a shirt, with plastic pistol at the beginning of the measurement (a), after 15 minutes (b) and after 30 minutes (c).

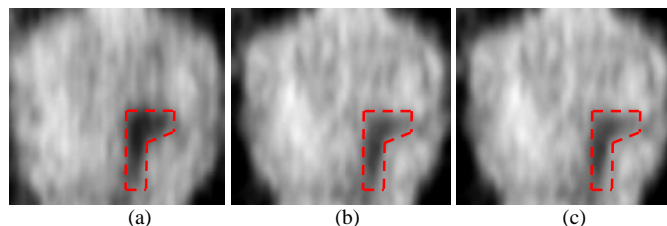


Fig. 12. THz images presenting a man wearing a shirt, with plastic pistol and metal knife at the beginning of the measurement (a), after 15 minutes (b) and after 30 minutes (c).

Results presented in Figs. 9 – 12 show that the concealed object can be easily detected by an analysis of anomalies in the THz and MWIR images. Moreover, the comparative assessment of images acquired in 5 minute time intervals indicates that objects' sharpness in the image is decreasing with time. Contrast of the concealed object decreased during the experiment. This is a consequence of a direct contact between the body and the object and a heat transfer between them. Both objects endeavour to achieve thermal equilibrium. Temperature of the human body remains constant, therefore, temperature of the concealed object increases during the experiment.

The ability to detect the concealed object with the infrared and terahertz cameras became less effective during the experiment and depended on the observed objects' temperature. Comparison of the images indicated that in the case of the terahertz images the contrast between the concealed object and the body was higher than in the case of MWIR images and did not decrease rapidly with time.

Below we present the analysis of dependencies between temperatures of the body and the objects, spectral range and pixels intensity. In order to present the numbers in a transparent manner, pixel values have been normalized using the following equation:

$$I_n(x, y) = \frac{I(x, y)}{\max(I)}, \quad (9)$$

where $I_n(x, y)$ is the value of a normalized pixel, $\max(I)$ is the maximum pixel value in the image, and $I(x, y)$ is the value of a pixel before normalization.

The presented results correspond to the theoretical analysis in Section 2. The values of the average temperature and pixel intensity determined for each ROI at equal time intervals corresponded to the change in CP value at each time.

Table 3 presents the change in normalized pixel intensity and temperatures measured using the thermocouples at the beginning and end of the measurement session.

TABLE III
CHANGES IN NORMALIZED PIXEL INTENSITY AND CONTACT TEMPERATURES

| | | shirt, pistol | shirt, knife |
|--------------------------------------|--------|---------------|--------------|
| Normalized pixel intensity of object | THz | 8.1% | 8.9% |
| | MWIR | 17.8% | 26.1% |
| Contact temperature | Object | 2.2 K | 3.0 K |
| | Body | 1.0 K | 0.9 K |

The change in the normalized pixel intensity of the object was the difference between the mean value of pixel intensities of a

selected region of interest at the beginning and end of the experiment. The selected region of interest was a 3×3 window of the image presented in Fig. 13.

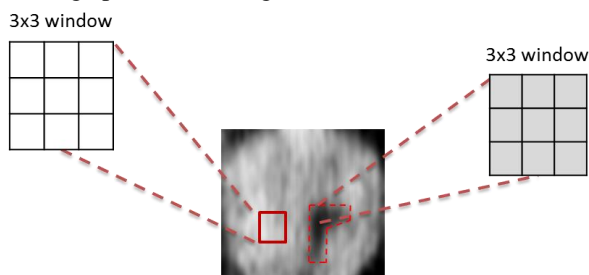


Fig.13. Regions of interest used to estimate the pixel values.

Analysis of the results presented in Table 3 indicates that greater changes in pixel intensities and temperatures were noticed for the metal knife than the metal pistol. The changes in pixel intensities were less than 10% and did not affect the observer’s ability to determine the object’s location. It should be noted that observer’s eye is not sensitive to absolute values but to relative values of magnitude between the region of interest and the neighbouring area. The values of the relative differences of pixel intensities are presented in Table 4.

TABLE IV
RELATIVE DIFFERENCES IN PIXEL VALUES OF REGION OF INTERESTS IN THE IMAGES

| | | shirt, pistol [%] | shirt, knife [%] |
|---|------|-------------------|------------------|
| Difference between the intensity of the hidden object and the clothing area | THz | 57.13 | 52.89 |
| | MWIR | 14.52 | 13.79 |

The measured values of the contact temperatures and normalized pixel intensity for two types of objects hidden under a shirt are presented in Fig. 14.

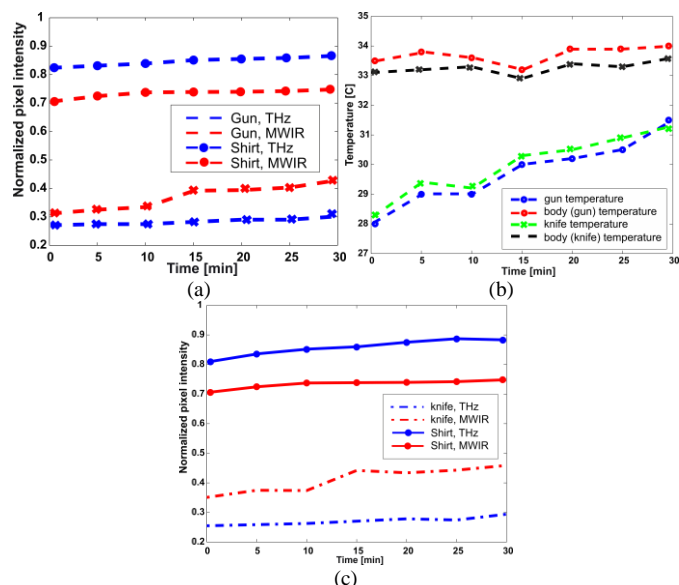


Fig. 14. The metal pistol hidden under a shirt (a) normalized pixel intensity; the metal knife hidden under a shirt (b) normalized pixel intensity; (c) contact temperature of objects (knife and pistol) and the body.

A very important physical aspect that may affect the ability of imagers to detect an object is the contact between hidden object, human body and clothing. The heat exchange described by Fourier’s law occurs only when the two bodies are directly connected with each other. While in the case of the human body and the object the condition is satisfied, loose clothing may not perfectly adhere to the object and the heat transfer may not be perfect. The adhesion of the clothing and the object has great significance. This problem had particular importance for the imaging of objects within the infrared range. When the contact between the object and the clothing is not uniform, the concealed object is visualized uniformly and its shape may not be correctly detected. This situation is presented in Fig. 15.

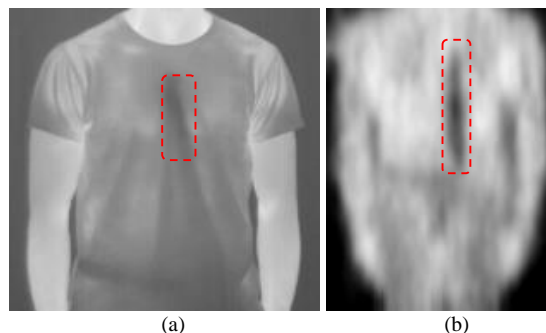


Fig. 15. Images presenting the object placed on the human body covered with loose clothing (a) MWIR image, (b) THz image.

It should be noted that terahertz imagers operate in shorter distances than MWIR imagers. Real distance of THz camera imaging used during the experiment was between 3 m and 9 m. Experiments conducted at a distance of over 6 m indicated that small items (knife, pistol) were undetectable. Longer distances do not allow for real observations and for effective detecting of such small objects.

VI. SUMMARY

The process of a hidden object’s detection has different physical sense in terahertz and infrared ranges. Terahertz cameras can visualize a hidden object mainly due to a non-zero transmission through clothing. Infrared cameras cannot utilize this property because the transmission of radiation from this range through clothing is negligible. However, by an analysis of anomalies of the temperature distribution on the clothing surface we can reveal the object.

Results from the comparative studies of passive imaging of hidden objects in terahertz and mid-wavelength infrared indicated several aspects that may influence the overall performance. The spectral range determines the radiation transmittance through clothing and the maximum spatial resolution of the imager. In this paper we presented how the transmittance changes within spectral range and how it depends on the fabric’s composition and thickness. The major conclusion is that fabric plays a key role; however, the results indicate a significant difference between the transmittance in the infrared and terahertz bands. The greater value of transmittance within the terahertz range is often compensated by the higher spatial resolution, greater range of imaging and thermal sensitivity of the infrared imager.

The experiments showed that the changes in the temperature values of the human body and the concealed object affect the detection ability of imagers operating in both the terahertz and infrared ranges. A summary of the presented studies showing the most important parameters from the point of view of object detection is presented in Table 5.

TABLE V
SUMMARY OF COMPARATIVE STUDIES OF TERAHERTZ AND MID-WAVELENGTH INFRARED PASSIVE IMAGING OF CONCEALED OBJECTS

| Parameter | terahertz | mid-wavelength infrared |
|--|-----------|-------------------------|
| Transmission through clothing | high | low |
| Time stability of imaging | high | medium |
| Image resolution | low | high |
| Contact between the object and clothes | important | not important |
| Identification of a person carrying the object | no | no |
| Range of imaging | low | high |

REFERENCES

[1] L. Kaufman, J. W. Carlson, "An evaluation of airport x-ray backscatter units based on image characteristics," *Journal of Transportation Security*, vol. 4, no. 1, pp. 73-94, Mar. 2011.

[2] Y. S. Lee, "Principles of Terahertz Science and Technology," New York: Springer, 2008.

[3] X Zhang, X. Jingzhou, "Introduction to THz Wave Photonics," New York: Springer, 2010.

[4] P. H. Siegel, "Terahertz technology," *IEEE Transactions Microw. Theory*, vol. 50, no. 3, pp. 910-928, Mar. 2002.

[5] R. Appleby, H.B. Wallace, "Standoff detection of weapons and contraband in the 100 GHz to 1 THz region," *IEEE Transactions on antennas and propag.*, vol. 55, no. 11, pp. 2944-2956, Nov. 2007.

[6] K. B. Cooper, R. J. Dengler, N. Lombart, B. Thomas, G. Chattopadhyay, P. H. Siegel, "THz Imaging Radar for Standoff Personnel Screening," *IEEE Transactions on terahertz Sci. and Technol.*, vol. 1, no. 1, pp. 169 – 182, Sept. 2011.

[7] R. Woodward, "Terahertz technology in global homeland security," *Proc. SPIE*, 5781, 2005.

[8] A. Rogalski, F. Sizov, "Terahertz detectors and focal plane arrays," *Opto-electronics Rev.*, vol. 19, no. 3, pp. 346-404, Oct. 2011.

[9] D. Mittleman, "Sensing with Terahertz Radiation," Berlin: Springer Verlag, 2003.

[10] D. Dragoman, M. Dragoman, "Terahertz fields and applications," *Prog. Quantum Electronics.*, vol. 28, no. 1, pp. 1-66, Jan. 2004.

[11] C. Jansen, S. Wietzke, O. Peters, M. Scheller, N. Vieweg, M. Salhi, N. Krumbholz, C. Jördens, T. Hochrein, M. Koch "Terahertz imaging: applications and perspectives," *Appl. Optics.*, vol. 49, no. 19, pp. E48-E57, May 2010.

[12] B. B. Hu, M. C. Nuss, "Imaging with terahertz waves," *Opt. Lett.*, vol. 20, no. 16, pp. 1716-1718, Apr. 1995.

[13] R. Appleby, R.N. Anderton, "Millimeter-Wave and Submillimeter-Wave Imaging for Security and Surveillance," In *Proceedings of IEEE*, 95, pp. 1683 – 1690, 2007.

[14] M. Kowalski, N. Palka, M. Piszczek, M. Szustakowski, "Hidden Object Detection System Based on Fusion of THz and VIS Images," *Acta Phys. Pol. A.*, vol. 124, no. 4, pp. 490-493, Sept. 2013.

[15] H. L. Hackforth, "Infrared Radiation," Warsaw: WNT, 1963.

[16] Y. Luo, W. Huang, "Attenuation of terahertz transmission through rain," *Optoelectronics Lett.*, vol. 8, no. 4, pp. 310-313, Aug. 2012.

[17] A. Rogalski, "History of infrared detectors," *Opto-electronics Rev.*, vol. 20, no. 3, pp. 279-308, Sept. 2012.

[18] M.C. Kemp, "Millimetre wave and terahertz technology for the detection of concealed threats: a review," in *Proceedings of IEEE Infrared and Millimeter Waves*, pp. 647 – 648, 2007.

[19] A H Lettington, Q H Hong, "An objective MRTD for discrete infrared imaging systems," *Meas. Sci. Technol.*, vol. 4, pp. 1106–1110, Apr. 1993.

[20] M. Planck, "The Theory of Heat Radiation," P. Blakiston's Son & Co, 1914.

[21] J. H. Lienhard IV, J. H. Lienhard V, "A heat transfer textbook, Cambridge: Phlogiston Press Cambridge, 2008.

[22] T. S. Hartwick, D. T. Hodges, D. H. Barker, F. B. Foote, "Far infrared imagery," *Appl. Optics*, vol. 15, no. 8, pp. 1919-22, May 1976.

[23] J. E. Bjamason, T. L. J. Chan, A. W. M. Lee, M. A. Celis, E. R. Brown, "Millimeter-wave, terahertz, and mid-infrared transmission through common clothing," *Appl. Phys. Lett.*, vol. 85, no. 4, pp. 519 – 521, Apr. 2004.

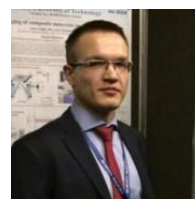
[24] <http://Teraview.com>

[25] <http://Bruker.com>

[26] M. Kowalski, M. Kastek, M. Walczakowski, N. Palka, M. Szustakowski (2015) Passive imaging of concealed objects in terahertz and long-wavelength infrared. *Appl. Optics*, vol. 54, No. 13, pp. 3826-3833, May 2015.

[27] <http://www.digitalbarriers.com/products/thruvision/>

[28] <http://Flir.com>



Marcin Kowalski is an assistant professor in the Institute of Optoelectronics at the Military University of Technology. He received the M.Sc. degree in electronics and telecommunications and a PhD degree in optoelectronics, both from the Military University of Technology, Warsaw, Poland in 2010 and 2014, respectively. After receiving the M.Sc. degree he joined the Military University of Technology as a Ph.D. student. His current research efforts focus on multispectral imaging systems and image processing and optical encryption.



Mariusz Kastek received a MSc degree in electronics (with a focus in optoelectronics) and a PhD degree in optoelectronics, both from the Military University of Technology, Warsaw, Poland, in 1993 and 2002, respectively. Since 1996 he has been working at the Institute of Optoelectronics, MUT. His main scientific interest is focused on multispectral and hyperspectral detection in infrared. He is an author of over 40 articles and 80 conferences publications. He is regular member of SPIE since 2001.